The Journal of Agricultural Science

cambridge.org/ags

Comparison of four upscaling methods to drive instantaneous evapotranspiration to daily values for maize in two climatic regions in China

Climate Change and Agriculture Research Paper

Cite this article: Wang X *et al* (2024). Comparison of four upscaling methods to drive instantaneous evapotranspiration to daily values for maize in two climatic regions in China. *The Journal of Agricultural Science* **162**, 539–552. https://doi.org/10.1017/S0021859624000637

Received: 21 June 2024
Revised: 18 September 2024
Accepted: 22 September 2024
First published online: 13 November 2024

Keywords:
crop coefficient method; direct canopy resistance method; evaporative fraction method

Corresponding author:
Haofang Yan;
Email: yanhaofangyhf@163.com

Xuanxuan Wang[1], Biyu Wang[1], Haofang Yan[1,3], Chuan Zhang[2], Hexiang Zheng[4], Guoqing Wang[3], Jianyun Zhang[3], Rongxuan Bao[1], Run Xue[2], Yudong Zhou[1], Jun Li[2], Rui Zhou[1], Bin He[5], Beibei Hao[5] and Yujing Han[1,5]

[1]Research Centre of Fluid Machinery Engineering and Technology, Jiangsu University, Zhenjiang 212013, China; [2]School of Agricultural Equipment Engineering, Jiangsu University, Zhenjiang 212013, China; [3]State Key Laboratory of Hydrology-Water Resources and Hydraulic Engineering, Nanjing Hydraulic Research Institute, Nanjing 210029, China; [4]Institute of Pastoral Hydraulic Research, China Institute of Water Resources and Hydropower Research, Hohhot 010020, China and [5]National-Regional Joint Engineering Research Center for Soil Pollution Control and Remediation in South China, Guangdong Key Laboratory of Integrated Agro-environmental Pollution Control and Management, Institute of Eco-environmental and Soil Sciences, Guangdong Academy of Sciences, Guangzhou 510650, China

Abstract

Accurately converting satellite instantaneous evapotranspiration (λET_i) over time to daily evapotranspiration (λET_d) is crucial for estimating regional evapotranspiration from remote sensing satellites, which plays an important role in effective water resource management. In this study, four upscaling methods based on the principle of energy balance, including the evaporative fraction method (*Eva-f* method), revised evaporative fraction method (*R-Eva-f* method), crop coefficient method (K_c-ET_0 method) and direct canopy resistance method (*Direct*-r_c method), were validated based on the measured data of the Bowen ratio energy balance system (*BREB*) in maize fields in northwestern (NW) and northeastern (NE) China (semi-arid and semi-humid continental climate regions) from 2021 to 2023. Results indicated that *Eva-f* and *R-Eva-f* methods were superior to K_c-ET_0 and *Direct*-r_c methods in both climatic regions and performed better between 10:00 and 11:00, with mean absolute errors (*MAE*) and coefficient of efficiency (ε) reaching <10 W/m^2 and > 0.91, respectively. Comprehensive evaluation of the optimal upscaling time using global performance indicators (*GPI*) showed that the *Eva-f* method had the highest *GPI* of 0.59 at 12:00 for the NW, while the *R-Eva-f* method had the highest *GPI* of 1.18 at 11:00 for the NE. As a result, the *Eva-f* approach is recommended as the best way for upscaling evapotranspiration in NW, with 12:00 being the ideal upscaling time. The *R-Eva-f* method is the optimum upscaling method for the Northeast area, with an ideal upscaling time of 11:00. The comprehensive results of this study could be useful for converting λET_i to λET_d.

Introduction

Understanding the regional water consumption and distribution plays an essential role in indicating crop water consumption and determining irrigation strategies (Ma *et al*., 2021; Disasa *et al*., 2024). Evapotranspiration (*ET*), equivalent form of the latent heat flux (λET), contributes significantly to the energy balance of farmed surfaces (Gao *et al*., 2018; Yan *et al*., 2018; Wang *et al*., 2024b), and is a key consideration for addressing a number of scientific and engineering issues, such as the hydrological cycles, climate change and carbon cycle (Ma *et al*., 2019; Xu *et al*., 2020; Liu *et al*., 2022; Lakhiar *et al*., 2024).

Farmland *ET* is estimated by several methods such as water balance (Choudhury *et al*., 2013; Jiang *et al*., 2014), lysimeters (Evett *et al*., 2012) and micrometeorological methods such as eddy covariance (Hossen *et al*., 2011; Yang *et al*., 2016) and Bowen ratio energy balance (Zhang *et al*., 2010; Pozníková *et al*., 2018; Yan *et al*., 2023; Li *et al*., 2024). However, the limitations of typical observation approaches include poor spatial representation, expensive installations, and only providing point measurements (Liu *et al*., 2012b).

In recent decades, remote sensing *ET* retrieval based on the combination of satellite remote sensing data and the land surface energy model has become an increasingly important area of research, as it can provide spatial distributions of surface information, solve the problem of bad spatial representativeness of the methods for point scale, and provide an effective way of calculating *ET* (Jung *et al*., 2010; Miralles *et al*., 2011; Mu *et al*., 2011; Zhang *et al*., 2019).

Nevertheless, remotely sensed data-based *ET* estimate algorithms can only compute an instantaneous energy budget at the time of the satellite overpass, which is not able to meet the requirements of *ET* on daily as well as longer time scale in practical applications (Delogu *et al.*, 2012; Liu *et al.*, 2017). Accurate daily *ET* can provide important guidance for water resources management, hydrological cycle studies and establishment of rational irrigation schedules (Tang *et al.*, 2013). It is, therefore, necessary to develop temporal upscaling methods in order to upgrade *ET* from an instantaneous to a daily scale (Jiang *et al.*, 2021), which may be an effective way to address the problem that remote sensing only provides a basic instantaneous estimate of *ET*, and this scaling-up relationship should be investigated and demonstrated through studies that primarily use localized (*in situ*) observations. In addition, the applicability of the upscaling approach to different ecosystems should be assessed, especially in water resources studies (Van Niel *et al.*, 2012).

Most of the existing upscaling methods in practice are developed based on daily stability or regularity properties in instantaneous *ET* estimation models (Chávez *et al.*, 2008; Cammalleri *et al.*, 2014). Relating daily *ET* (λET_d) to a component that can be almost constant during the day or throughout a diurnal cycle is crucial to the development of different upscaling methods (Farah *et al.*, 2004; Liu *et al.*, 2012a). The factor can be stated as the ratio of an hourly computable reference variable to instantaneous *ET* (λET_i) at a given time of day (Van Niel *et al.*, 2012; Tang *et al.*, 2013; Cammalleri *et al.*, 2014). Several methods, including the evapotranspiration fraction method, the crop coefficient method, the canopy resistance method, the Katerji Perrier method, the advective drought method, and the daily sinusoidal function, can be used to estimate λET_d based on the assumption that the diurnal course of *ET* is similar to that of the solar irradiance.

The evaporative fraction (E_f), defined as the ratio between latent heat flux and available energy at the surface, is an important parameter that reflects the distribution of available energy at the surface and explains the components of the energy budget (Shuttleworth *et al.*, 1989). Many studies have been conducted to test the validity of the evaporative fraction method (*Eva-f* method) utilizing local available energy observations and the self-preservation assumption that E_f remains roughly constant throughout the day. Tang *et al.* (2013) and Zhang *et al.* (2017) found that the *Eva-f* method accurately estimates λET_d for winter wheat and summer maize in Northern China and semiarid northwest China, respectively. However, previous studies have revealed that a range of environmental factors has an impact on the assumption of self-preservation (Farah *et al.*, 2004; Gentine *et al.*, 2007; Xu *et al.*, 2015; Wandera *et al.*, 2017). The E_f during the daytime is largely time related and depends strongly on soil moisture effectiveness, canopy cover, developmental stage, relative humidity, and the biological characteristics of vegetation in an area (Gentine *et al.*, 2007; Hoedjes *et al.*, 2008), while the surface energy budget affects the microclimate of the vegetation canopy (Hossen *et al.*, 2011). These variable environmental factors may lead to inaccuracies in λET_d estimates when using the *Eva-f* method. As a result, there is no consensus on the overall trend of daytime E_f fluctuations, which may vary from site to site (Van Niel *et al.*, 2011). Tang *et al.* (2013) and Van Niel *et al.* (2012) implied that the E_f is more variable under cloudy conditions compared to clear sky conditions. The daily shape of E_f depends on atmospheric forcing and surface conditions (Gentine *et al.*, 2007); the E_f typically remains constant in the morning and increases sharply in the afternoon (Gentine *et al.*, 2007; Delogu *et al.*, 2012). Gentine *et al.* (2007) and Hoedjes *et al.* (2008) found that the E_f fluctuates more in humid areas, whereas the *Eva-f* method performs best in arid areas. In addition, the E_f was also affected by effective energy, which varied little in areas with high effective energy during the day (Li *et al.*, 2008). When the leaf area index is large, the E_f is less stable for the same amount of soil moisture (Gentine *et al.*, 2007). Allen *et al.* (2007) noted a consistent decrease in hourly E_f for mowed grass, whereas sugarbeet had a significant increase in E_f in the afternoon. Chemin and Alexandridis (2001) suggested that assuming soil heat flux (G) equal to 0 may significantly improve the accuracy of the *Eva-f* method for calculating λET_d because the G is a low percentage of the surface energy balance and always varies with soil thermal properties and soil moisture. Therefore, a revised evaporative fraction method (*R-Eva-f* method) was developed to calculate the λET_d using a modified evaporative fraction (RE_f), which is the proportion of λET to net radiation (R_n). Suleiman and Crago (2004) found that the *R-Eva-f* method is more effective for extrapolating λET_d from time-by-time measurements in grasslands. Chávez *et al.* (2008) showed that the *R-Eva-f* method overestimates λET_d in maize and soybean fields.

Allen *et al.* (2007) found that the crop coefficient (K_c), which is the ratio of *ET* to reference evapotranspiration (ET_0), is almost constant at low daylight frequencies, which applied to *ET* magnification and was named the crop coefficient method (K_c-ET_0 method). Several experiments have successfully estimated the λET_d from instantaneous values using the K_c-ET_0 method, which considers the influence of atmospheric characteristics (Delogu *et al.*, 2012; Xu *et al.*, 2015; Zhang *et al.*, 2017). The K_c-ET_0 method performed well over agricultural irrigated areas (Allen *et al.*, 2007), but poorly over bare soil where *ET* decreased rapidly (Colaizzi *et al.*, 2006).

Furthermore, the direct canopy resistance method (*Direct-*r_c method) was developed by Farah *et al.* (2004) to estimate the λET_d from the λET_i based on a diurnal fluctuation of canopy resistance (r_c).The effectiveness of the *Direct-*r_c method has been validated by numerous studies (Tang *et al.*, 2017; Zhang *et al.*, 2017; Yan *et al.*, 2022b). Tang *et al.* (2017) and Yan *et al.* (2022b) reported that the *Direct-*r_c method did not yield a much closer scaled λET_d when utilizing varied r_c as opposed to fixed r_c. They also noted that the assumption that the r_c would be virtually constant during the day was dubious and that more research was necessary.

A number of comparative analyses have also been carried out to evaluate the precision and suitability of various upscaling methods. As for the comparison of the *ET* scaling up methods based on E_f, K_c and r_c, Colaizzi *et al.* (2006) and Xu *et al.* (2015) showed that the estimated λET_d based on the *Eva-f* method fitted measured values better for non-vegetated land cover, while the K_c-ET_0 method and *Direct-*r_c method had the best performance during the season of vegetation growth. Chávez *et al.* (2008) found that the K_c-ET_0 method performed better under uniform vegetation cover, whereas the *R-Eva-f* method overestimates λET_d for both corn and soybean fields. Yan *et al.* (2022b) noted that in circumstances where there is a significant departure from reference grass, the K_c-ET_0 method may not perform well. Tang *et al.* (2013) used eddy-correlation data from northern China to assess the efficacy of four upscaling methods, and showed that the K_c-ET_0 method was the most accurate in the clear and partly cloudy skies. Another comparative study based on four upscaled methods was also conducted in Australia, and the *Direct-r*$_c$ method was used to calculate λET_d for maize and canola crops, with a high degree of consistency with eddy-correlation systems (Liu *et al*., 2012a). Zhang *et al*. (2017) found that the *Eva-f* and K_c-ET_0 methods gave the best performance when using instantaneous values from 11:00 to 15:00. Yan *et al*. (2022b) reported that the *Eva-f* and *R-Eva-f* methods gave the best performance when using instantaneous values for the time period 11:00–14:00.

Previous studies have shown that the accuracy and applicability of different upscaling methods are affected by factors such as ecosystem, location, instantaneous time of upscaling and meteorological data. The performance of the above upscaling methods at instantaneous time may be different under different satellite traversal times, climatic conditions and vegetation growth conditions. Thus, the objectives of this study were (1) to evaluate the performances of the four scaling methods (*Eva-f*, *R-Eva-f*, K_c-ET_0 and *Direct-r*$_c$ method) in estimation of the λET_d from λET_i for maize grown in two climatic regions (semi-arid and semi-humid continental climate); (2) to comprehensively evaluate the optimal scale-up times of the four models by adopting global performance indicators (*GPI*); (3) to analyse the differences of these methods under two climatic regions and (4) to recommend proper approaches for estimating λET_d and the optimal upscaling time for two climatic regions.

Materials and methods

Field observations

The experimental data used in this study were obtained from two long-term automatic meteorological stations in northwestern and northeastern China. The experiment in northwestern China (NW) was conducted in a maize field located at Ordos city (39° 53′ N, 109°60′ E, 1456 m a.s.l.) from May 2022 to September 2023. It is a semi-arid temperate continental monsoon area with abundant sunshine resources, average hours of sunshine are more than 3000 h per year, the average annual temperature is 12.9 °C, the average annual precipitation ranges from 190 to 300 mm, the evaporation of free water surface is 1500 mm and the frost-free period is 150 days. The soil texture is primarily sandy soil, with an average soil bulk density and field water-holding capacity of 1.60 g/cm^3 and 24.7%, respectively. The experiment in northeastern China (NE) was conducted in a maize field located at Harbin city (45°38′ N, 126°22′ E, 140 m a.s.l.) from May 2021 to October 2022. It has a temperate semi-moist continental monsoon climate, with rainfall mainly occurring from June to September, and the average annual precipitation ranges from 500 to 600 mm. The average annual temperature is about 6.9°C, with the highest and lowest average monthly temperatures occurring in July (23.7°C) and January (−13.5°C), respectively. The soil texture is primarily loamy, with an average bulk density and field water-holding capacity of 1.35 g/cm^3 and 32.0%, respectively. The location and precipitation information for both sites are shown in Fig. 1. The precipitation data were obtained from the Geographic Data Sharing Infrastructure (GDSI), Global Resource Data Cloud (www.gis5g.com).

Two sets of Bowen ratio energy balance (*BREB*) observation systems were installed in the centre of the maize fields at the NW and NE China experimental stations (Yan *et al*., 2022b). The study fields were surrounded by other similar crops and the installation heights of the probes used to observe the

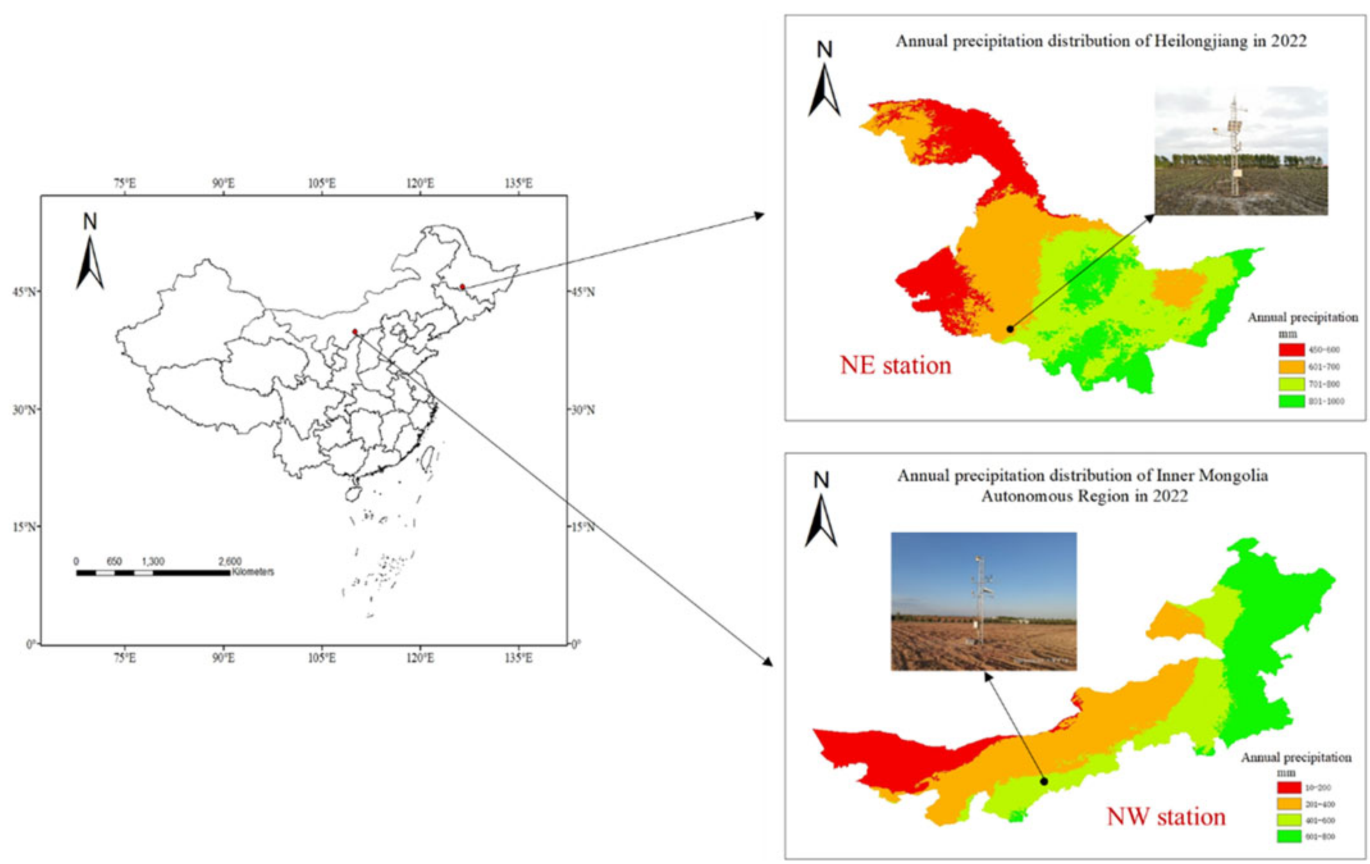

Figure 1. Locations of the two climatic regions of northern China.

https://doi.org/10.1017/S0021859624000637 Published online by Cambridge University Press

temperature and humidity were low (50–100 cm above the canopy), so adequate fetch length (> 100–200 m) can be provided (Yan *et al.*, 2021). Net radiation (R_n) of maize fields at two sites was measured by CNR-4 sensors (Kipp and Zonen, Netherlands) at 4 m for NW and 3 m for NE above the ground; wind speed (u) was measured by three-cup anemometers, A100L2 (MetOne, USA, with an accuracy of ±0.12 m/s), at 6 m for NW and 4 m for NE above the ground; and the air temperature (T_a) and relative humidity (RH) were measured with HMP155A sensors (Vaisala, Finland, accuracy ±0.1°C for T_a and ±2% for RH) at 3 and 4 m above the ground for NW station, and at 3.5 and 4.5 m above the ground for NE station for the Bowen ratio energy balance (*BREB*) method; the volumetric soil water content (*VWC*) was measured by five TDR-315H sensors (Acclima, USA) at depths of 20, 40, 60, 80 and 100 cm at the centre of the field at NW station; four TDR-315H sensors (Acclima, USA) were used in NE station to measure the *VWC* at 5, 10, 20 and 100 cm; the soil heat flux (G) measurements in both stations were carried out using soil heat flux panels HFP01-L10 (Campbell Scientific, USA) and rainfall (P) was measured using TE525MM (Campbell Scientific, USA). All sensors were connected to a CR1000 data logger (Campbell Scientific, USA), with an average sampling frequency of every 10 min (Jiang *et al.*, 2024). The accuracy of all sensors was verified prior to installation. Data are missing from 12 May 2022 to 29 May 2022 at the NW station and from 21 August 2022 to 14 September 2022 at the NE station due to instrument failure. The date format used was ISO 8601 time format (https://en.wikipedia.org/wiki/ISO_8601).

Scaling up methods

Eva-f method

The evaporative fraction (*Eva-f*) method can be expressed as (Sugita and Brutsaert, 1991):

$$E_f = \frac{\lambda ET_i}{(R_n - G)_i} \tag{1}$$

$$\lambda ET_d = E_f (R_n - G)_d \tag{2}$$

where E_f is the evaporative fraction at a certain hourly time, λET_i and λET_d are the latent heat flux at time i and total daytime, respectively (W/m^2). R_n and G are the net radiation and soil heat flux (W/m^2) and λ is the latent heat of vaporization (J/kg). The subscripts i and d express the instantaneous time of day and total daytime values, respectively.

R-Eva-f method

The revised evaporative fraction (*R-Eva-f*) method estimating λET_d from λET_i was proposed on the assumption that the daily mean value of the soil heat flux (G) in *Eva-f* method is zero (Chemin and Alexandridis, 2001) and expressed as follows:

$$RE_f = \frac{\lambda ET_i}{R_{ni}} \tag{3}$$

$$\lambda ET_d = RE_f \times R_{nd} \tag{4}$$

where RE_f is the ratio of λET_i and R_{ni} at a certain hourly time, other symbols have the same meanings as in (Eqns (1) and (2)).

K_c-ET_0 method

The crop coefficient (K_c-ET_0) method to estimate λET_d from λET_i based on the crop coefficient (K_c) can be expressed as follows (Colaizzi *et al.*, 2006):

$$\lambda ET_{0i} = \frac{\Delta_i (Rn - G)_i + \rho_{ai} C_p VPD_i u_{2i}/208}{\Delta_i + \gamma_i (1 + 0.34 u_{2i})} \tag{5}$$

$$K_{ci} = \frac{\lambda ET_i}{\lambda ET_{0i}} \tag{6}$$

$$\lambda ET_d = K_{ci} \times \lambda ET_{0d} \tag{7}$$

where K_c is the crop coefficient at a certain hourly time, λET_0 is the latent heat flux from the reference crops (W/m^2), Δ is the slope of the saturation vapour pressure curve (kPa/°C), ρ_a is the air density (kg/m^3), C_p is the specific heat of dry air at constant pressure (J/kg/K), VPD is the vapour pressure deficit (kPa), γ is the psychrometric constant (kPa/°C), and u_2 is the wind speed at 2 m height (m/s), the subscripts i and d express the instantaneous time of day and total daytime values, respectively.

Direct-r_c method

The direct canopy resistance (*Direct-r_c*) method to estimate λET_d from λET_i based on r_c can be expressed as follows (Malek *et al.*, 1992):

$$r_c = r_{ai} \times \left[\left(\frac{\Delta_i (R_n - G)_i + \dfrac{\rho_a C_p VPD_i}{r_{ai}}}{\lambda ET_i} - \Delta_i \right) \frac{1}{\gamma_i} - 1 \right] \tag{8}$$

$$\lambda ET_d = \frac{\Delta_d (R_n - G)_d + \dfrac{\rho_a C_p VPD_d}{r_{ad}})}{\Delta_d + \gamma_d (1 + \dfrac{r_c}{r_{ad}})} \tag{9}$$

where r_a is the aerodynamic resistance (s/m), r_c is the canopy resistance (s/m), the subscripts i and d express the instantaneous time of day and total daytime values, respectively.

The value of r_a was calculated by (Thom, 1972):

$$r_a = \frac{\ln \dfrac{z - d}{z_0} \ln \dfrac{z - d}{z_{0h}}}{\kappa^2 u_z} \tag{10}$$

where z is the height of wind measurements (m), d is the zero plane displacement height (m) estimated as $d = 0.67h_c$, h_c is the mean height of the crop (m), z_0 is the roughness length governing momentum transfer (m) calculated as $z_0 = 0.123h_c$, z_{0h} is the roughness length governing transfer of heat and vapour (m) computed as $z_{0h} = 0.1z_0$, u_z is the wind speed at height z (m/s), and κ is the von Karman constant (= 0.41).

Evapotranspiration measurements

One of the standard techniques for measuring λET indirectly is the Bowen ratio energy balance (*BREB*) method (Pozníková *et al.*, 2018; Yan *et al.*, 2022a). The *BREB* determines the latent heat and sensible heat fluxes based on the rearrangement of the simplified surface energy balance equation given by (Heilman and Brittin, 1989):

$$\lambda ET_i = \frac{R_n - G}{1 + \beta} \tag{11}$$

$$\beta = \frac{H}{\lambda ET_i} = \gamma \frac{\Delta T}{\Delta e} \tag{12}$$

where β is the Bowen ratio, ΔT is the air temperature gradient and Δe is the actual vapour pressure gradient. The measured λET_d were computed by the sum of λET_i which was obtained using the *BREB* method based on the hourly meteorological data from 8:00 to 16:00 for both areas. To control the measurement quality, the λET results were ignored when β was close to -0.75 (Ohmura, 1982).

Performance evaluation

The relative performance of the four upscaling methods was evaluated using the statistical indices, including coefficient of determination (R^2), mean absolute error (*MAE*), relative root mean absolute error (*RRMSE*) and coefficient of efficiency (ε).

$$MAE = \frac{1}{n} \sum_{i=1}^{n} |E_i - O_i| \tag{13}$$

$$RRMSE = \frac{\sqrt{\frac{1}{n} \sum_{i=1}^{n} (E_i - O_i)^2}}{\overline{O}} \tag{14}$$

$$\varepsilon = 1.0 - \frac{\sum_{i=1}^{N} |O_i - E_i|}{\sum_{i=1}^{N} |O_i - \bar{O}|} \tag{15}$$

where E_i and O_i represent the estimated and observed values, respectively, n is the total sample number and $\overline{O}$ is the mean of observed values. R^2 represents the degree of replication of the model to the observed value. The higher the value of R^2 is, the better the performance is. Both *RRMSE* and *MAE* values are range from 0 (perfect fit) to ∞ (worst fit). ε is dimensionless,

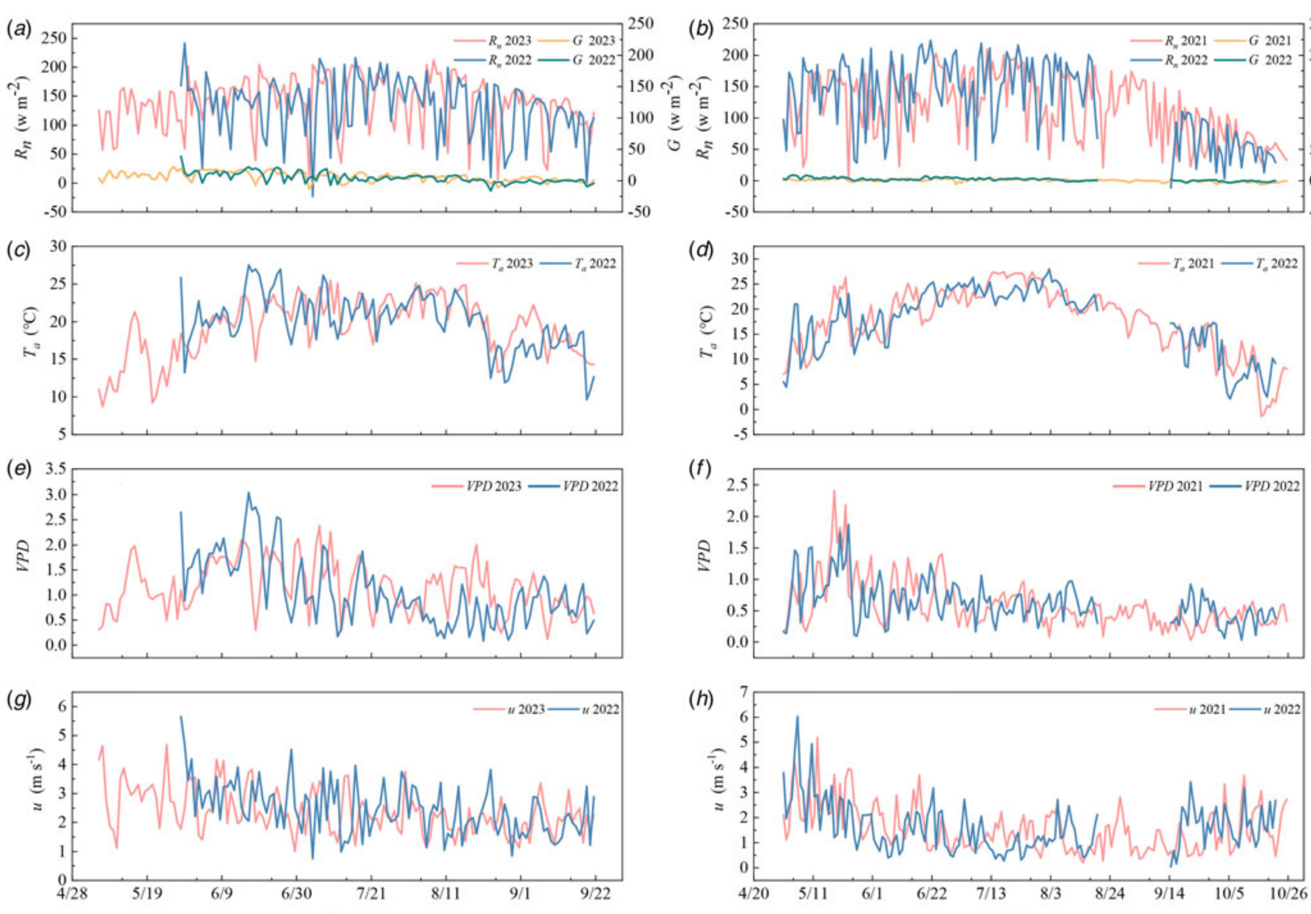

Figure 2. Variations of meteorological data during maize growing periods in two climatic regions. R_n is the net radiation, G is the soil heat flux, T_a is the air temperature, *VPD* is the vapour pressure deficit and u is the wind speed. (a), (c), (e) and (g) for northwestern China, (b), (d), (f) and (h) for northeastern China.

https://doi.org/10.1017/S0021859624000637 Published online by Cambridge University Press

which ranges from 0 (worst fit) to 1 (perfect fit) (Yan *et al.*, 2019; Zhao *et al.*, 2023; Wang *et al.*, 2024a).

The optimal upscaling methods based on the four accuracy evaluation indexes differed at different fertility stages, but also the optimal upscaling moments were not exactly the same, and thus the global performance indicators (*GPI*) was introduced to comprehensively evaluate the optimal upscaling times of the four models (Despotovic *et al.*, 2015). The calculation formula is as follows:

$$GPI_i = \sum_{j=1}^{4} \alpha_j (y_j - y_{ij}) \tag{16}$$

As for indicators of R^2 and ε, a_j is equal to −1, while as for other indicators, a_j is equal to 1, y_j is the median scale value of the index j and y_{ij} is the scale value of the index j in the model i. The higher the *GPI* value is, the higher the accuracy of the model is.

Results

Meteorological conditions

The observed meteorological data during the growing periods of maize in two climatic regions are shown in Fig. 2. For the NW station, the net radiation (R_n) in 2022 (from 12 May to 26 Sep) ranged from −22.8 to 241.6 W/m^2, with average value of 132.0 W/m^2, and the corresponding values ranged from 6.96 to 213.0 W/m^2, with average value of 139.0 W/m^2 in 2023 (from 6 May to 22 Sep). The soil heat flux (G) in 2022 ranged from −16.2 to 39.1 W/m^2, with average value of 4.33 W/m^2, and the corresponding value ranged from −13.5 to 22.2 W/m^2, with average value of 6.23 W/m^2 in 2023.

The air temperature (T_a) in 2022 ranged from 8.71 to 27.5 °C, with average value equalled 19.8 °C, while T_a in 2023 ranged from 8.75 to 25.5 °C, with average value equalled 19.2 °C. The vapour pressure deficit (*VPD*) in 2022 ranged from 0.09 to 3.04 kPa, with average value equalled 1.06 kPa, while *VPD* in 2023 ranged from 0.12 to 2.38 kPa, with average value equalled 1.15 kPa. The wind speed (u) had mean values of 2.45 m/s for 2022 and 2.38 m/s for 2023, with maximum values of 5.65 and 4.68 m/s.

For the NE station, the R_n in 2021 (from 1 May to 26 Oct) ranged from 3.27 to 209.7 W/m^2, with average value of 116.3 W/m^2 and the corresponding values ranged from −11.7 to 223.7 W/m^2, with average value of 126.5 W/m^2 in 2022 (from 1 May to 22 Oct). The G in 2021 ranged from −6.07 to 4.94 W/m^2, with average value of 0.35 W/m^2, and the corresponding values ranged from −3.17 to 8.71 W/m^2, with average value of 1.94 W/m^2 in 2022. The T_a in 2021 ranged from −1.34 to 27.4 °C, with average value equalled 17.7 °C, while T_a in 2022 ranged from 2.12 to 28.0 °C, with average value equalled 17.7 °C. The VPD in 2021 ranged from 0.03 to 2.41 kPa, with average value equalled 0.59 kPa,

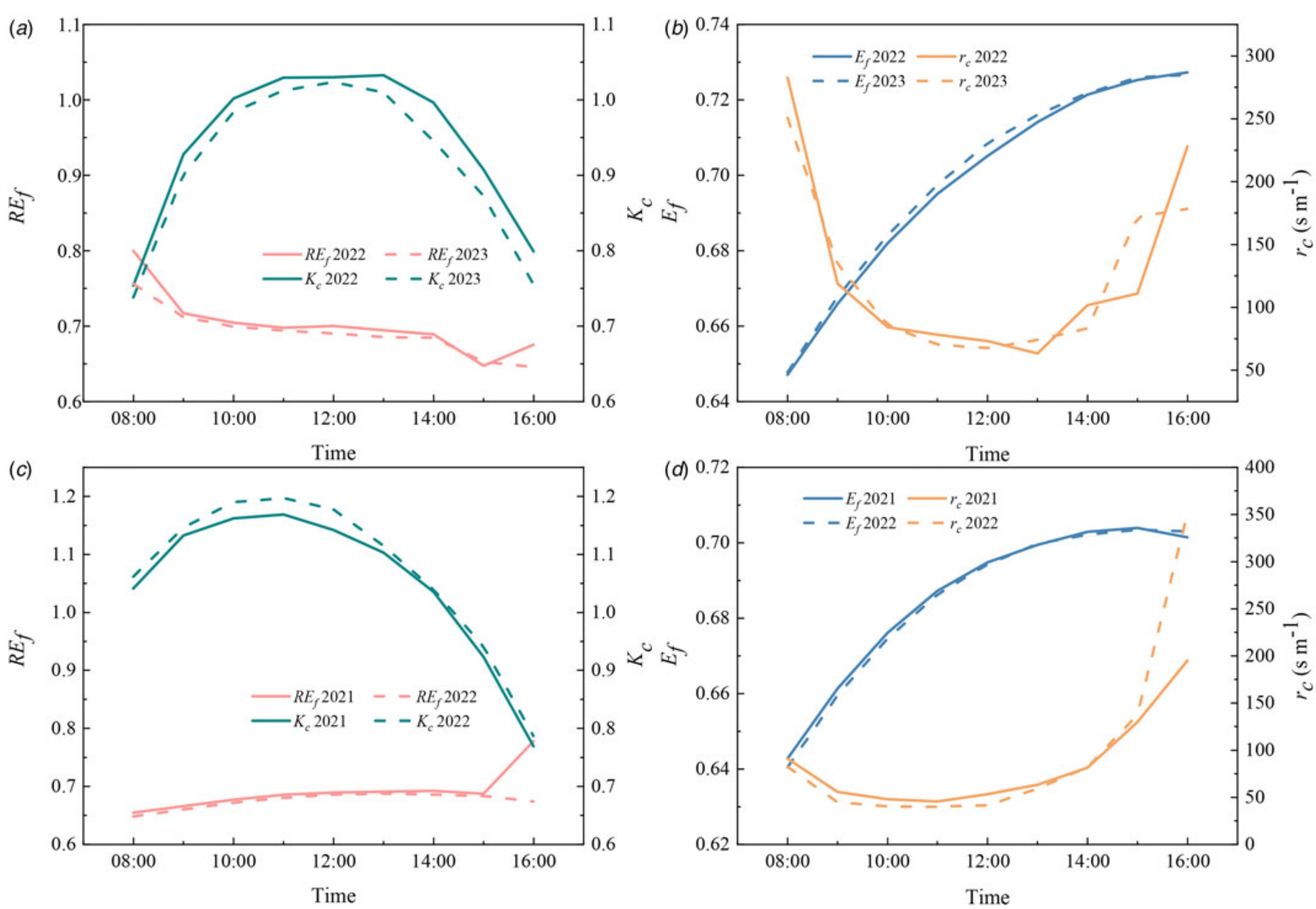

Figure 3. Hourly variations in calculated evaporative fraction (E_f), revised evaporative fraction (RE_f), crop coefficient (K_c) and canopy resistance (r_c) for maize. (a), (b) for northwestern China and (c), (d) for northeastern China.

https://doi.org/10.1017/S0021859624000637 Published online by Cambridge University Press

while VPD in 2022 ranged from 0.03 to 1.88 kPa, with average value equalled 0.63 kPa. The u had mean values of 1.55 m/s for 2021 and 1.62 m/s for 2022, with maximum values of 5.18 and 6.03 m/s.

Validity of the constancy of the upscaling factors

Figure 3 is the diurnal variations of the evaporative fraction (E_f), revised evaporative fraction (RE_f), crop coefficient (K_c), and canopy resistance (r_c) obtained by averaging the parameters during 2022–2023 and 2021–2022 maize growing seasons in NW and NE, respectively. The amplitude of variations in the E_f, RE_f, K_c and r_c were similar over NW and NE. Specifically, the E_f showed a slightly increasing trend and ranged from 0.6 to 0.8 over both areas, which attributed the reason to the dry weather conditions (Hoedjes *et al*., 2008; Yang *et al*., 2013). The diurnal pattern of RE_f remained constant for most of the time except for the period close to sunrise and sunset, which may be due to lower available energy flux to drive ET in the early morning and the late afternoon (Yan *et al*., 2022b).

The parameter K_c exhibited a typical down-concave shape throughout the day, with relatively sharp variations in the early morning and late afternoon, and reached a maximum near midday. The turbulent exchange was intense, especially after sunrise and before sunset. The latent heat flux varied greatly, and the susceptibility of wind speed was obvious. The ET capacity and ET intensity of the subsurface were affected, so that K_c fluctuated greatly. However, the calculation of the E_f ignored these effects and assumed that the impedance was constant, and thus the fluctuation was small. The trend of K_c in this study was consistent with previous studies (Liu *et al*., 2012a; Yan *et al*., 2022b). However, the magnitude of K_c was usually higher than E_f, which was related to soil moisture stress and vegetation cover (Zhang *et al*., 2017).

The trend of r_c exhibited a dramatically declining tendency in the early morning and late afternoon, while maintaining steady for the majority of the day, with a mean of 125 s/m in the NW, and 91 s/m in the NE. The rapid increase in r_c was partly due to the high atmospheric stability in the late afternoon, which reduced the soil water content and the overall resistance to evapotranspiration in the maize field. On the other hand, because the R_n decreased rapidly in the afternoon, but the decrease of G lagged behind that of R_n, so the calculated effective energy was smaller than that of the actual effective energy, and the inverse calculation of r_c using the P-M formula was on the large side, and the estimated λET_d was on the small side. The daily variations of E_f and K_c were mainly affected by stomatal regulation and the diurnal pattern of T_a, VPD and relative humidity, which has

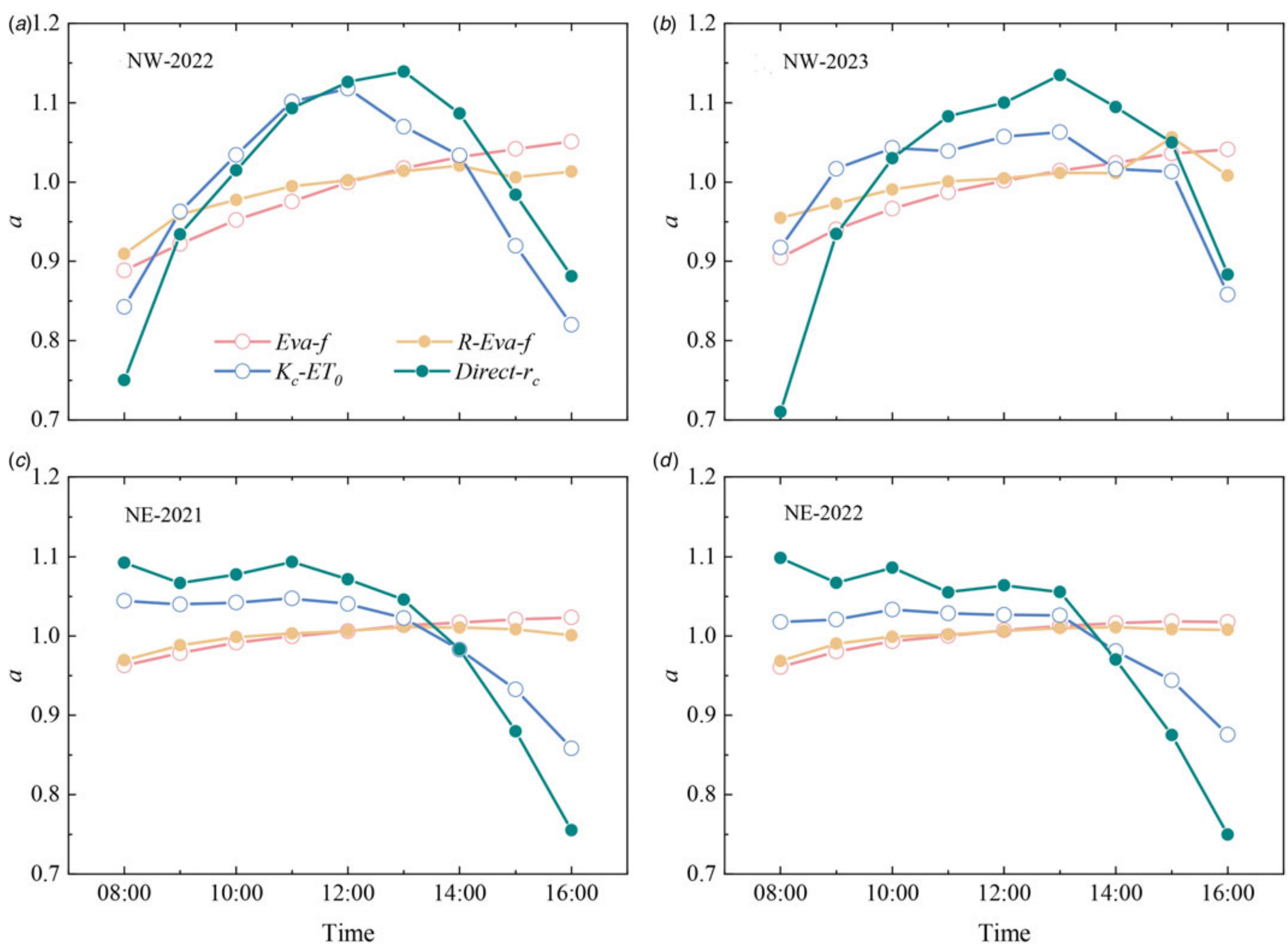

Figure 4. Slopes (α) obtained by comparing the simulated daily evapotranspiration (λET_d) of the four upscaling methods with the measured λET_d based on the Bowen ratio energy balance system (*BREB*) method. (a), (b) For northwestern China and (c), (d) for northeastern China.

https://doi.org/10.1017/S0021859624000637 Published online by Cambridge University Press

strong effects on stomatal resistance (Yang *et al.*, 2013; Liu *et al.*, 2020).

Performance of the four upscaling methods

Based on λET_d estimated by the *BREB* method, the efficacy of four upscaling methods (*Eva-f*, *R-Eva-f*, K_c-ET_0 and *Direct-*r_c methods) for estimating λET_d of NW and NE maize based on λET_i for the time period 08:00–16:00 was verified. The λET_i between 08:00 and 16:00 was chosen because it coincided with the time when the majority of satellites emerge over the study area and the upscaling factors are relatively stable.

The correlations between the estimated and measured λET_d at different hourly periods (08:00–16:00) for the four methods are shown in Figs 4 and 5. The slopes (α) of the fits of the four scaling methods at the two stations showed different degrees of intraday decreasing or increasing, which indicated that the four scaling methods had great variability in the calculation results for estimating λET_d using λET_i at different moments. The slopes of the measured and estimated λET_d by *Eva-f* and *R-Eva-f* methods for both climatic zones were the closest to 1 during the 10:00–14:00 time period, were the smallest during the 08:00–10:00 time period, were the largest during the 14:00–16:00 time period, and then increased, but the slopes did not vary much from one time period to the next. The slopes of the K_c-ET_0 and *Direct-*r_c methods varied drastically, with different trends in magnitude. In 2022, the slopes in NW region increased and then decreased from 08:00 to 16:00, and were the closest to 1 for the time period 09:00–11:00 and 13:00–15:00, respectively. In 2023, the slopes in NW region increased from 08:00 to 16:00, and were the closest to 1 for the time period 09:00–11:00 and 13:00–15:00, respectively. The slopes in NW region showed an increase and then a gradual stabilization and then a decrease from 08:00 to 16:00, and was the closest to 1 in the 09:00–15:00 time period with similar variations in 2021 and 2022, and both showed gradual decrease, and a rapid decrease after 13:00 which upscales the estimated λET_d larger than the measured value. The coefficients of determination (R^2) of the estimation results of the four methods were mostly located near 1, indicating a strong correlation between the measured and estimated λET_d. The simulation results of the four methods were the closest to each other during the 10:00–14:00 time period. In terms of the fitted R^2, all four methods showed high in midday and low in morning and afternoon. Previous studies found a minor divergence between measured λET_d and the estimations based on midday λET_i (Hoedjes *et al.*, 2008; Zhang *et al.*, 2017; Jiang *et al.*, 2021).

The mean absolute error (*MAE*) and relative root mean squared error (*RRMSE*) of the estimated λET_d calculated by

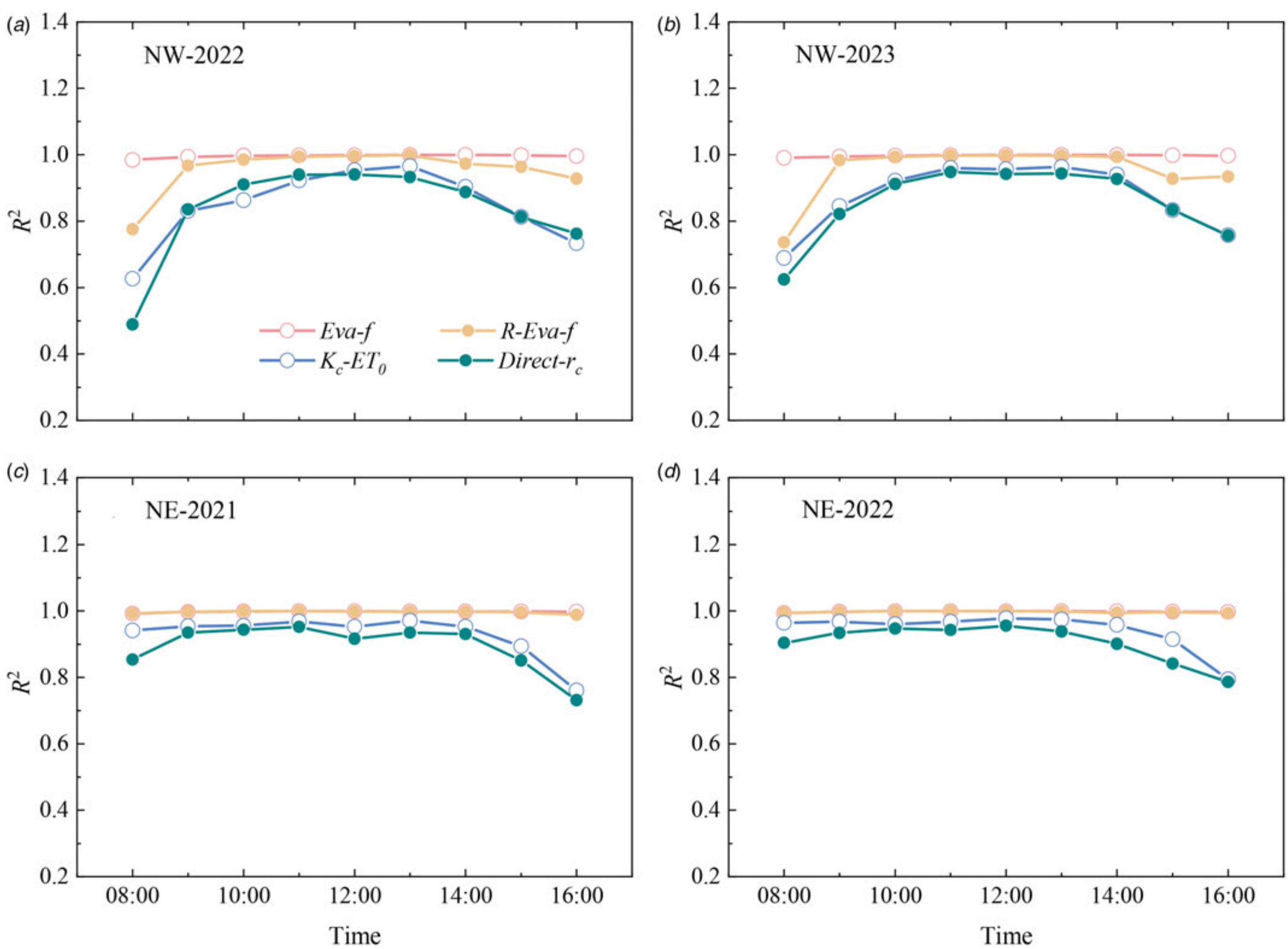

Figure 5. Coefficients of determination (R^2) obtained by comparing the simulated daily evapotranspiration (λET_d) of the four upscaling methods with the measured λET_d based on the Bowen ratio energy balance system (*BREB*) method. (a), (b) For northwestern China and (c), (d) for northeastern China.

four methods varied greatly as shown in Figs 6 and 7. The results of the *MAE* and *RRMSE* exhibited similar performance, with the *Eva-f* and *R-Eva-f* methods having the smallest *MAE* and *RRMSE* during the study periods. The K_c-ET_0 and *Direct*-r_c methods performed unstable, with a slightly higher *MAE* and *RRMSE* than the *Eva-f* and *R-Eva-f* methods. For the K_c-ET_0 method, the *MAE* and *RRMSE* showed different performance for NW and NE, which the minimum values appeared when the λET_i was used at 14:00 and 13:00 for NW and NE, respectively. The results of *MAE* and *RRMSE* illustrated that the *Direct*-r_c method exhibited similar performance in NW and NE. The trend of *MAE* and *RRMSE* showed upward concave shape, which confirmed the underperformance for most time in NW and NE. During the day, the *MAE* and *RRMSE* of the *Eva-f* and *R-Eva-f* methods were generally consistent, with average values of less than 10.1 W/m^2 and 0.03. When using the λET_i from 9:00 to 15:00, the K_c-ET_0 and *Direct*-r_c methods had an average *MAE* of 27.3 W/m^2, which was considered satisfactory accuracy.

Moreover, diurnal variation of the efficiency coefficient (ε) of four methods was displayed in Fig. 8. The hourly variations of ε for the *Eva-f* and *R-Eva-f* methods changed slightly and the values were more stable for NE than for NW. For the K_c-ET_0 and *Direct*-r_c methods, the trend of ε curves showed clear similarities. For the NW station, the ε values of the K_c-ET_0 and *Direct*-r_c methods were lower when the λET_i in the morning was used, and remain around 0.6 for the rest of the day, but decreased obviously for the time period 10:00–14:00. For the NE station, the trend of ε curves sharply concaved down and attached the peak when the λET_i at 14:00 was used. Overall, the *Eva-f* method performed best and followed by the *R-Eva-f* method, with mean ε values less than 0.85 at all times; while the K_c-ET_0 and *Direct*-r_c methods performed worst in most cases. The mean ε values of the K_c-ET_0 and *Direct*-r_c method were only 0.55 and 0.46 for NW and 0.73 and 0.57 for NE, respectively.

From the above evaluation, it can be seen that not only the optimal upscaling methods based on the four accuracy evaluation indexes differed at different fertility stages, but also the optimal upscaling moments were not exactly the same, and thus the global performance indicators (*GPI*) was introduced to comprehensively evaluate the optimal upscaling times of the four models. Based on the four upscaling methods, the *GPI* of the calculated λET_d and measured values for different time intervals at the NW and NE stations were shown in Fig. 9. The larger the *GPI* value, the better the simulation performance. The four upscaling methods showed the ability to accurately simulate daily λET_d from 10:00 to 14:00, and the *Eva-f* and K_c-ET_0 methods were superior to the K_c-ET_0

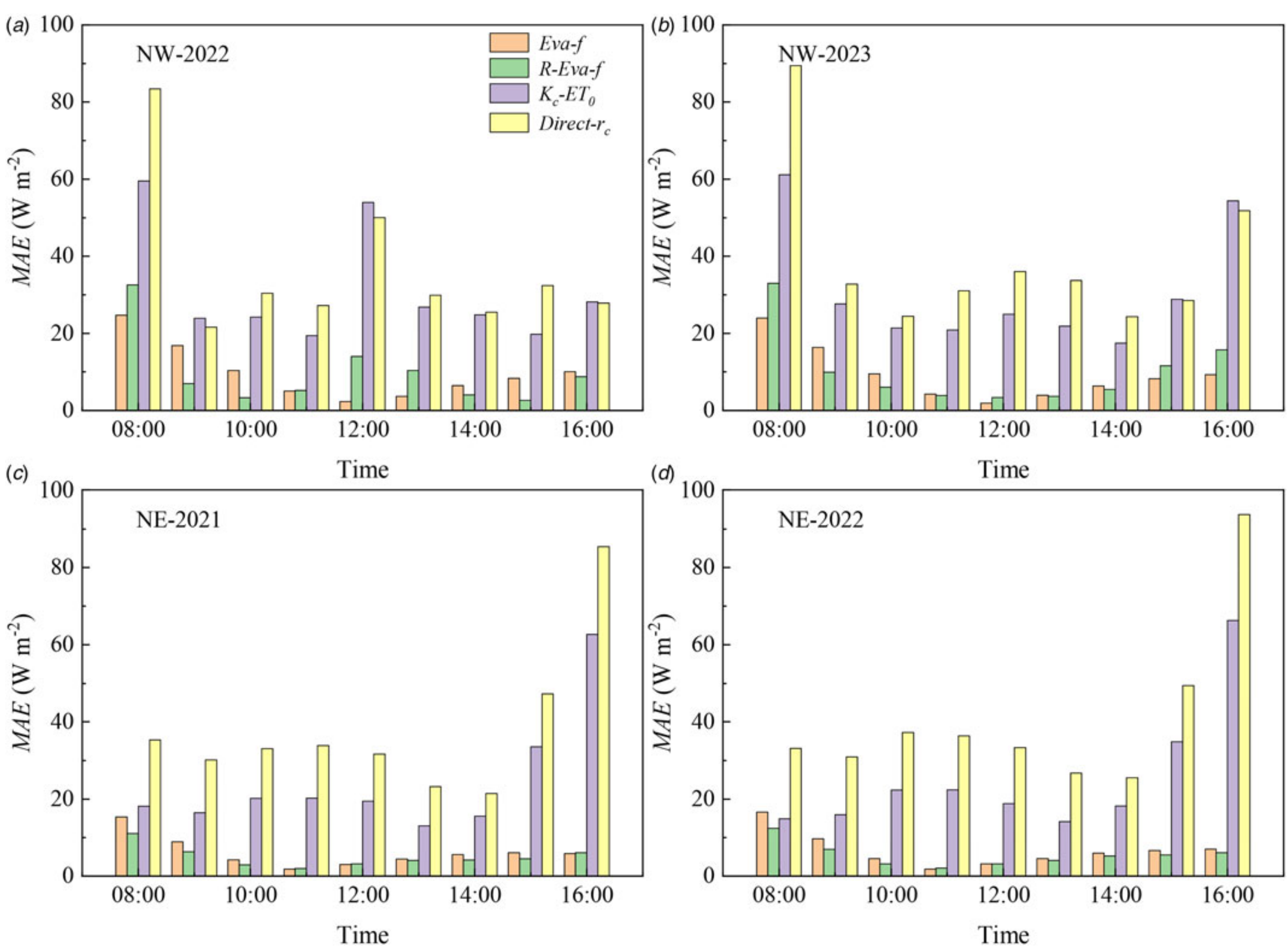

Figure 6. Mean absolute error (*MAE*) obtained by comparing the simulated daily evapotranspiration (λET_d) of the four upscaling methods with the measured λET_d based on the Bowen ratio energy balance system (*BREB*) method. (a), (b) For northwestern China and (c), (d) for northeastern China.

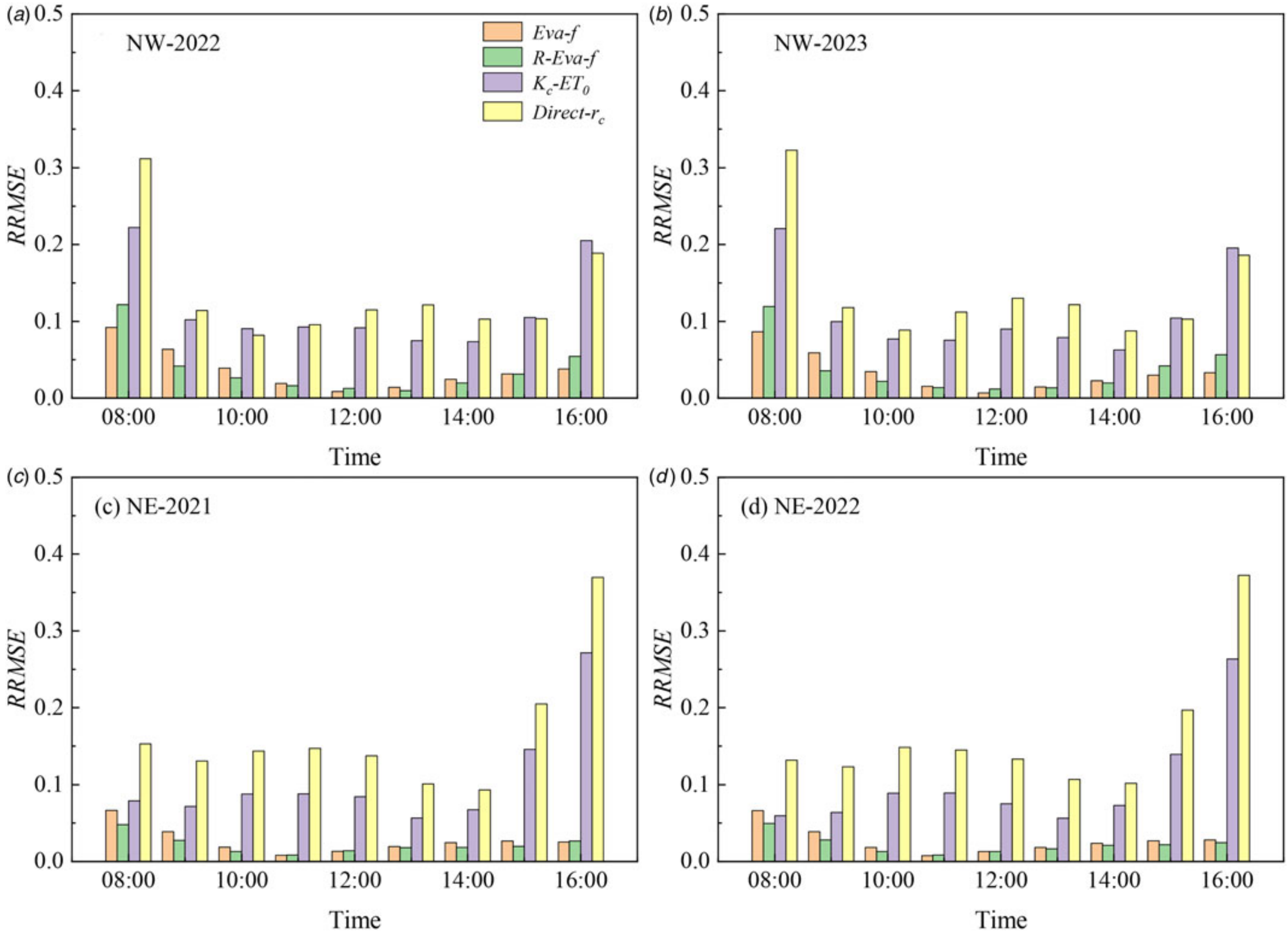

Figure 7. Relative root mean absolute error *(RRMSE)* obtained by comparing the simulated daily evapotranspiration (λET_d) of the four upscaling methods with the measured λET_d based on the Bowen ratio energy balance system (*BREB*) method. (a), (b) For northwestern China and (c), (d) for northeastern China.

and *Direct-*r_c methods. However, the *GPI* of the four methods decreased obviously when the λET_i in the morning and afternoon was used. Overall, the *Eva-f* method performed best at 12:00 for the NW station, with the mean *GPI* of 0.55 for two years. At the NE station, the *R-Eva-f* method performed best at 14:00, with the mean *GPI* of 1.04 for two years.

Discussion

The key parameters for upscaling methods (*Eva-f*, *R-Eva-f*, K_c-ET_0 and *Direct-*r_c method) showed different characteristics of variation and temporal representativeness. The results of this study showed that the E_f and RE_f in the process of estimating λET_i to λET_d changed slightly through the day, which is similar to the results of Zhang *et al.* (2017) on maize in north China. However, Yan *et al.* (2022b) showed that the E_f and RE_f showed an arch shape for a tea and wheat field during the day in southeast China. This difference may be due to the difference in meteorological factors, leaf area index and crop physiological mechanisms. It may also be due to the fact that solar radiation was lower in the morning and afternoon, resulting in less available energy flux to drive *ET*. Thus, the results in the calculated E_f and RE_f were unstable in these time periods. The K_c displayed a somewhat concave-down shape through the day, with comparatively sharp variations in the early morning and late afternoon. The K_c was not only related to the crop type, but also closely related to the climatic conditions, volumetric soil water content, crop cultivation conditions, irrigation and drainage management in the study areas. It is difficult to use the same set of K_c variation rules to reflect the λET_d, so it is necessary to determine the K_c based on the actual conditions of the study areas to accurately estimate the λET_d (Bezerra *et al.*, 2012). The trend of r_c showed a typical concave-up shape through the day. Due to the problem of condensate re-evaporation after sunrise, the r_c values back-calculated with the P-M formula were too small or even less than 0,which was similar to the results of the previous study (Perez *et al.*, 2005). The r_c values appeared to be constant with a slight increase in shape for the time period 12:00–14:00, which was attributed to an increase in r_c due to partial stomatal closure at midday when the light was stronger (Allen *et al.*, 2006). The change of r_c were influenced by field climate, such as R_n, *VPD*, etc. (Liu *et al.*, 2020). The trend of r_c showed to sharply increase in the late afternoon. Specifically, on the one hand, crop stomatal conductance decreased with decrease in radiation intensity, so r_c increased rapidly near noon. In most cases, all four upscaling methods showed some degree of underestimation, with better performance during the middle of the day

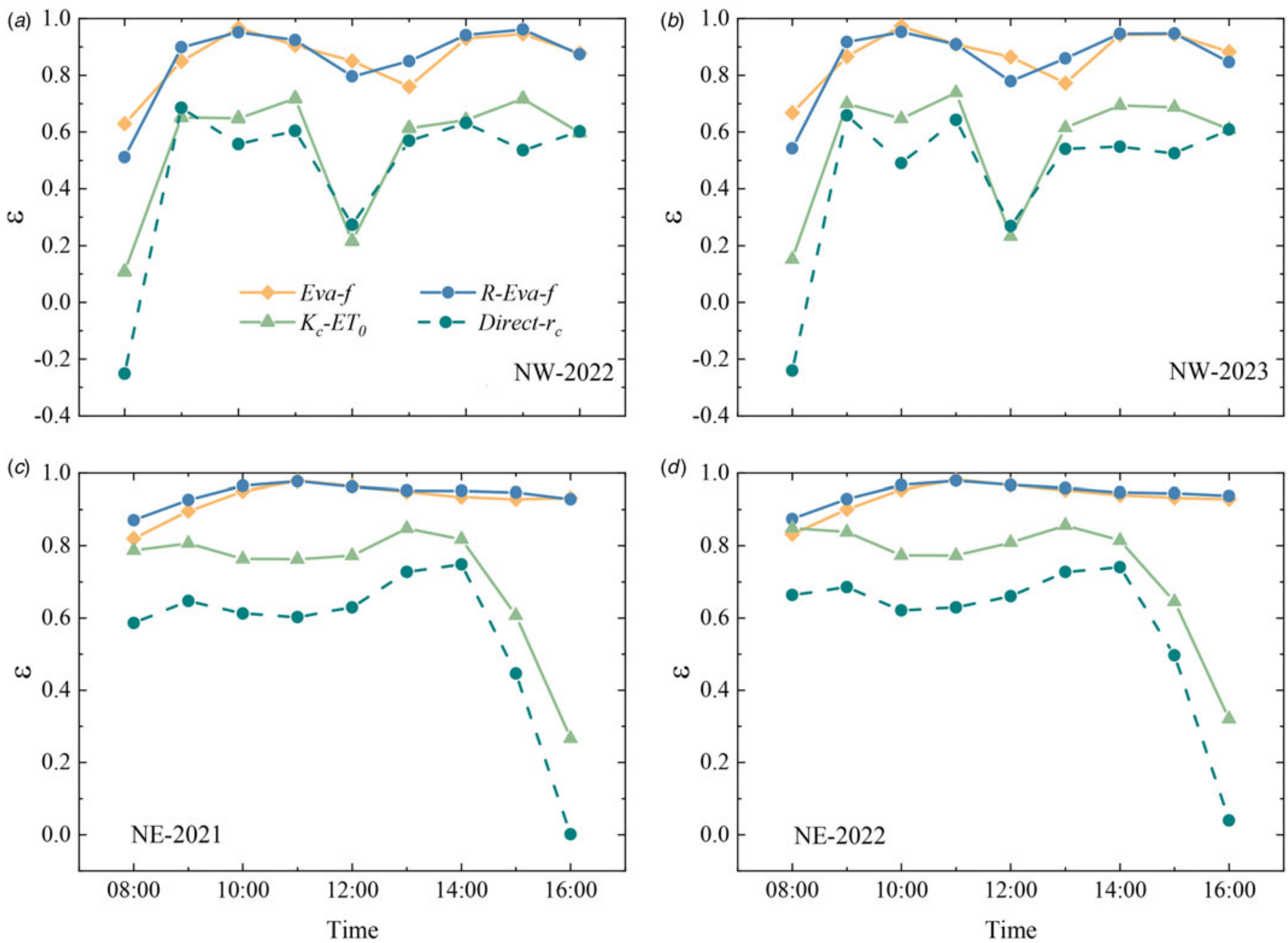

Figure 8. Coefficient of efficiency (ε) obtained by comparing the simulated daily evapotranspiration (λET_d) of the four upscaling methods with the measured λET_d based on the Bowen ratio energy balance system (*BREB*) method. (a), (b) For northwestern China and (c), (d) for northeastern China.

than in the morning and afternoon, which agreed with other research results (Tang and Li, 2017; Zhang *et al.*, 2017). The presence of clouds and energy conditions may be a potential reason for the underestimation of λET_d, (Delogu *et al.*, 2012; Tang *et al.*, 2017; Jiang *et al.*, 2018).

In this study, we found that the *Eva-f* method performed best for the time period 11:00–2:00 in both NW and NE stations. The *R-Eva-f* method performed best for the time period 10:00–11:00 for the NW station and for the time period 10:00–12:00 for the NE station. Yan *et al.* (2022b) and Liu (2021) concluded that the optimal upscaling time period of the *Eva-f* and *R-Eva-f* methods was from 09:00 to 15:00, particularly for instantaneous values between 11:00 and 14:00. In addition, Zhang *et al.* (2017) showed that the optimal upscaling moment of the *Eva-f* method was 14:00–15:00 on maize. The reason for this difference was mainly due to the difference in the geographical location of the study regions. The difference in sunrise and sunset times in different geographical locations led to the slight difference in optimal upscaling moment of the study regions. Liu *et al.* (2011) found that the K_c remained mostly constant during the reproductive period of wheat. The values in the morning (10:00–11:00) and afternoon (14:00–15:00) were the most similar to the daily average values, which were less than 1. Chávez *et al.* (2008) and Katimbo *et al.* (2022) found that the accuracy of estimating λET_d using the K_c-ET_0 method was not as good as the *Eva-f* method, but the accuracy of the estimation could be improved by using the K_c values during the midday. There was a clear intraday variation characteristic of K_c in this study. At the NW station, the fluctuation of K_c was smaller from 10:00 to 14:00. The fluctuation of K_c was smaller from 10:00 to 12:00 for the NE station. Thus, it was seen that the study of the optimal upscaling timing in different regions was an important prerequisite for the improvement of the estimation accuracy of λET_d by the K_c-ET_0 method. From the analysis of r_c, it was concluded that the r_c values for the time period 10:00–11:00 instead of daily average value were more effective in estimating λET_d for the NW station. At the NE station, the r_c for the time period 13:00–14:00 instead of daily value were more effective in estimating λET_d. This period coincided with the time of remote sensing satellite transit, and the time period (9:00–11:00) is the process of atmospheric stability changing from stable to unstable, which is in line with the condition of atmospheric neutral stability assumed by aerodynamic drag.

Taken together, both the *Eva-f* and *R-Eva-f* methods achieved good results in modelling λET_d from λET_i at most of the time. However, the *R-Eva-f* method was slightly inferior to the *Eva-f* method for two different climatic regions, and similar conclusions

https://doi.org/10.1017/S0021859624000637 Published online by Cambridge University Press

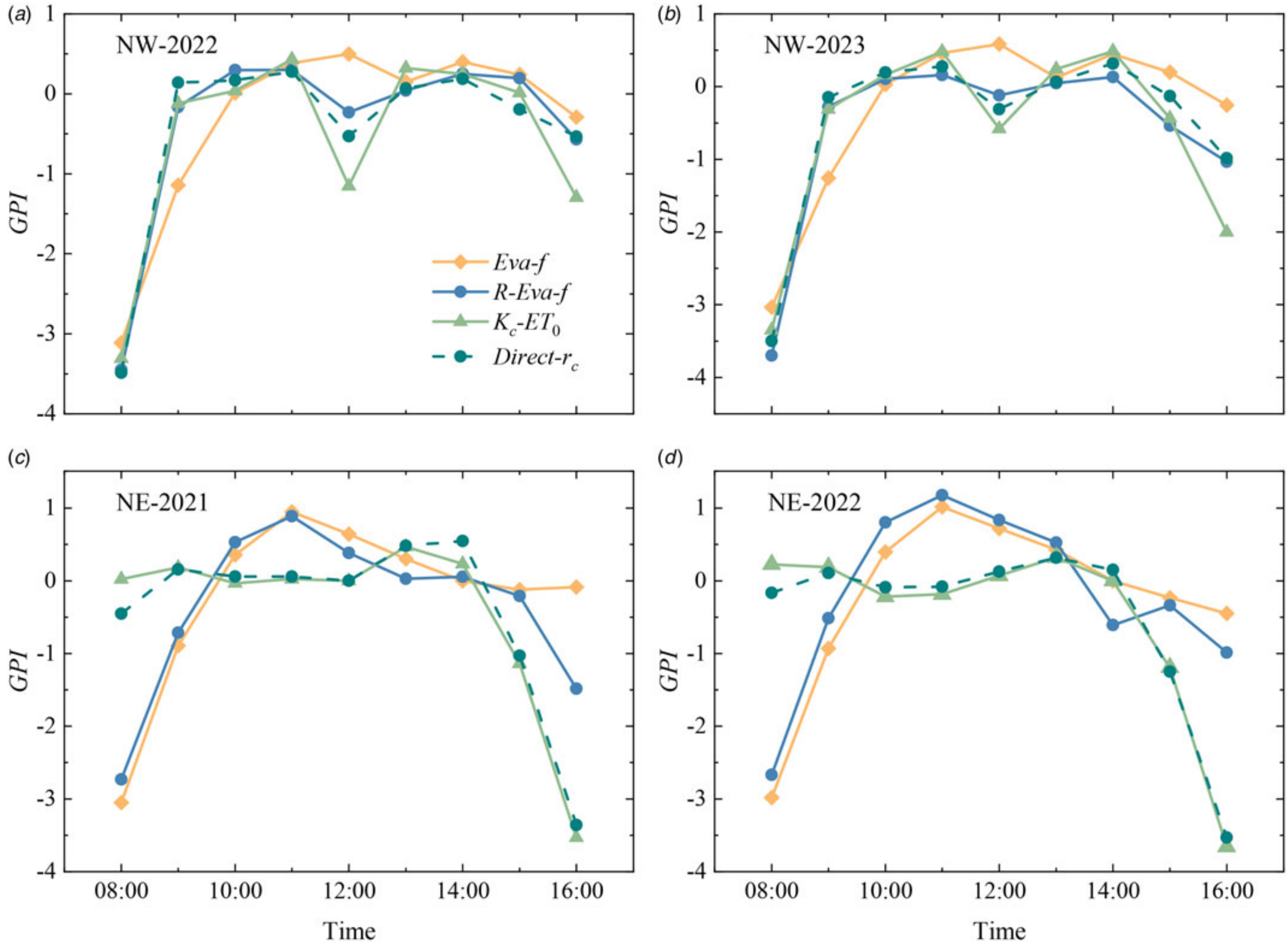

Figure 9. Global performance indicators (*GPI*) of four upscaling methods at different times. (a), (b) For northwestern China and (c), (d) for northeastern China.

were obtained by Yan *et al.* (2022b) for tea and wheat in southeast China. Liu (2021) reported the *Eva-f* method, which uses potential evapotranspiration and incoming shortwave radiation, outperformed the other methods for simulating daily series. Chen *et al.* (2013) and Jiang *et al.* (2021) concluded that the *R-Eva-f* method performed best for most ecosystems. This discrepancy was mainly due to errors in the observation of *G*, where the soil heat flux sensors were buried in the soil surface and were affected by changes in wind speed, soil properties and soil moisture. However, Cammalleri *et al.* (2014) pointed out that if the daily fluxes were for 24 h instead of just the daytime, the influence of *G* might not be as significant. Yang *et al.* (2013) showed that the diurnal pattern of K_c was strongly dependent on the leaf area index (*LAI*) and the K_c-ET_0 method may perform poorly at higher *LAI*, whereas Zhang *et al.* (2017) reported the performance of the K_c-ET_0 methods was good under various *LAI*. The *Direct*-r_c method showed poor estimation results in most intervals, which suggested the *Direct*-r_c method in extrapolating λET_i into λET_d may not be valid in this study and is no longer robust and universally applicable.

Conclusion

In this study, we evaluated four upscaling methods (*Eva-f*, *R-Eva-f*, K_c-ET_0 and *Direct*-r_c methods) performance in estimating λET_d from λET_i, using the measurements of λET_d by Bowen ratio energy balance system in two different climatic regions of Northwest and Northeast China based on the measured data from 2021 to 2023, and the following conclusions were drawn:

(1) The key parameters E_f, RE_f, K_c and r_c of λET_i to λET_d upscaling had obvious daily variation characteristics, and the overall trends were consistent in the two regions, with E_f and RE_f behaving more closely than K_c and r_c.

(2) The *Eva-f* and *R-Eva-f* methods were better than the other two methods (K_c-ET_0 and *Direct*-r_c methods) in all evaluation indexes, but the *R-Eva-f* method was slightly inferior to the *Eva-f* method due to the neglect of soil heat flux (*G*). Both the *Eva-f* and *R-Eva-f* methods were more suitable for the Northwest and Northeast regions.

(3) The time for λET_i had a significant effect on estimating λET_d by upscaling methods. Specifically, at the NW station, the *Eva-f* method gave the best scaling when λET_i at 12:00 was used, while at the NE station, the λET_d simulation had the highest accuracy using the *R-Eva-f* method when the λET_i at 11:00 was used.

(4) Therefore, it is recommended that the *Eva-f* method is the preferred method for upscaling evapotranspiration in the

Northwest region, with the moment of 12:00 being the optimal upscaling time. The *R-Eva-f* method is the best upscaling method for the Northeast region, with 11:00 being the optimal upscaling time.

Author contributions. Xuanxuan Wang, Biyu Wang, Haofang Yan, Chuan Zhang, Hexiang Zheng, Guoqing Wang, Jianyun Zhang and Bin He conceived and designed the study. Rongxuan Bao, Run Xue, Yudong Zhou, Jun Li, Rui Zhou, Beibei Hao and Yujing Han conducted data gathering. Xuanxuan Wang, Biyu Wang performed statistical analyses. Xuanxuan Wang, Biyu Wang and Haofang Yan wrote the article.

Funding statement. This study was financially supported by the National Key R&D Program (2021YFC3201103, 2023YFC3205701), the Natural Science Foundation of China (52121006, U2243228, 1509107, 42177065).

Competing interests. The authors declare that there is no conflict of interest, nor is there any commercial or competing interest, which is defined as a conflict of interest in connection with the work submitted.

Ethical standards. Not applicable.

References

Allen RG, Pruitt WO, Wright JL, Howell TA, Ventura F, Snyder R, Itenfisu D, Steduto P, Berengena J, Yrisarry JB, Smith M, Pereira LS, Raes D, Perrier A, Alves I, Walter I and Elliott R (2006) A recommendation on standardized surface resistance for hourly calculation of reference ETo by the FAO56 Penman–Monteith method. *Agricultural Water Management* **81**, 1–22.

Allen RG, Tasumi M, Morse A, Trezza R, Wright JL, Bastiaanssen W, Kramber W, Lorite I and Robison CW (2007) Satellite-based energy balance for mapping evapotranspiration with internalized calibration (METRIC) – applications. *Journal of Irrigation and Drainage Engineering* **133**, 395–406.

Bezerra BG, da Silva BB, Bezerra JRC, Sofiatti V and dos Santos CAC (2012) Evapotranspiration and crop coefficient for sprinkler-irrigated cotton crop in Apodi Plateau semiarid lands of Brazil. *Agricultural Water Management* **107**, 86–93.

Cammalleri C, Anderson MC and Kustas WP (2014) Upscaling of evapotranspiration fluxes from instantaneous to daytime scales for thermal remote sensing applications. *Hydrology and Earth System Sciences* **18**, 1885–1894.

Chávez JL, Neale CMU, Prueger JH and Kustas WP (2008) Daily evapotranspiration estimates from extrapolating instantaneous airborne remote sensing ET values. *Irrigation Science* **27**, 67–81.

Chemin Y and Alexandridis T (2001) Improving spatial resolution of ET seasonal for irrigated rice in Zhanghe. *The 22nd Asian Conference on Remote Sensing* 5, 9.

Chen H, Yang D and Lü H (2013) Comparison of temporal extrapolation methods for evapotranspiration over variant underlying croplands. *Transactions of the Chinese Society of Agricultural Engineering* **29**, 73–81.

Choudhury BU, Singh AK and Pradhan S (2013) Estimation of crop coefficients of dry-seeded irrigated rice-wheat rotation on raised beds by field water balance method in the Indo-Gangetic plains, India. *Agricultural Water Management* **123**, 20–31.

Colaizzi PD, Evett SR, Howell TA and Tolk JA (2006) Comparison of five models to scale daily evapotranspiration from one-time-of-day measurements. *Transactions of the ASABE* **49**, 1409–1417.

Delogu E, Boulet G, Olioso A, Coudert B, Chirouze J, Ceschia E, Le Dantec V, Marloie O, Chehbouni G and Lagouarde JP (2012) Reconstruction of temporal variations of evapotranspiration using instantaneous estimates at the time of satellite overpass. *Hydrology and Earth System Sciences* **16**, 2995–3010.

Despotovic M, Nedic V, Despotovic D and Cvetanovic S (2015) Review and statistical analysis of different global solar radiation sunshine models. *Renewable and Sustainable Energy Reviews* **52**, 1869–1880.

Disasa KN, Yan H, Wang G, Zhang J, Zhang C and Zhu X (2024) Projection of future precipitation, air temperature, and solar radiation changes in southeastern China. *Theoretical and Applied Climatology* **155**, 4481–4560.

Evett SR, Schwartz RC, Howell TA, Louis Baumhardt R and Copeland KS (2012) Can weighing lysimeter ET represent surrounding field ET well enough to test flux station measurements of daily and sub-daily ET? *Advances in Water Resources* **50**, 79–90.

Farah HO, Bastiaanssen WGM and Feddes RA (2004) Evaluation of the temporal variability of the evaporative fraction in a tropical watershed. *International Journal of Applied Earth Observation and Geoinformation* **5**, 129–140.

Gao X, Mei X, Gu F, Hao W, Gong D and Li H (2018) Evapotranspiration partitioning and energy budget in a rainfed spring maize field on the Loess Plateau, China. *Catena* **166**, 249–259.

Gentine P, Entekhabi D, Chehbouni A, Boulet G and Duchemin B (2007) Analysis of evaporative fraction diurnal behaviour. *Agricultural and Forest Meteorology* **143**, 13–29.

Heilman JL and Brittin CL (1989) Fetch requirements for Bowen ratio measurements of latent and sensible heat fluxes. *Agricultural and Forest Meteorology* **44**, 261–273.

Hoedjes JCB, Chehbouni A, Jacob F, Ezzahar J and Boulet G (2008) Deriving daily evapotranspiration from remotely sensed instantaneous evaporative fraction over olive orchard in semi-arid Morocco. *Journal of Hydrology* **354**, 53–64.

Hossen MS, Mano M, Miyata A, Baten MA and Hiyama T (2011) Surface energy partitioning and evapotranspiration over a double-cropping paddy field in Bangladesh. *Hydrological Processes* **26**, 1311–1320.

Jiang X, Kang S, Tong L, Li F, Li D, Ding R and Qiu R (2014) Crop coefficient and evapotranspiration of grain maize modified by planting density in an arid region of northwest China. *Agricultural Water Management* **142**, 135–143.

Jiang Y, Tang R, Jiang X and Li Z-L (2018) Impact of clouds on the estimation of daily evapotranspiration from MODIS-derived instantaneous evapotranspiration using the constant global shortwave radiation ratio method. *International Journal of Remote Sensing* **40**, 1930–1944.

Jiang L, Zhang B, Han S, Chen H and Wei Z (2021) Upscaling evapotranspiration from the instantaneous to the daily time scale: assessing six methods including an optimized coefficient based on worldwide eddy covariance flux network. *Journal of Hydrology* **596**, 126135.

Jiang J, Yan H, Zhang C, Wang G, Zhang J, Liang S and Deng S (2024) Simulation of greenhouse cucumber evapotranspiration based on canopy-air temperature difference. *Journal of Drainage and Irrigation Machinery Engineering* **42**, 532–540.

Jung M, Reichstein M, Ciais P, Seneviratne SI, Sheffield J, Goulden ML, Bonan G, Cescatti A, Chen J, de Jeu R, Dolman AJ, Eugster W, Gerten D, Gianelle D, Gobron N, Heinke J, Kimball J, Law BE, Montagnani L, Mu Q, Mueller B, Oleson K, Papale D, Richardson AD, Roupsard O, Running S, Tomelleri E, Viovy N, Weber U, Williams C, Wood E, Zaehle S and Zhang K (2010) Recent decline in the global land evapotranspiration trend due to limited moisture supply. *Nature* **467**, 951–954.

Katimbo A, Rudnick DR, Liang W-Z, DeJonge KC, Lo TH, Franz TE, Ge Y, Qiao X, Kabenge I and Nakabuye HN (2022) Two source energy balance maize evapotranspiration estimates using close-canopy mobile infrared sensors and upscaling methods under variable water stress conditions. *Agricultural Water Management* **274**, 107972.

Lakhiar IA, Yan H, Zhang J, Wang G, Deng S, Bao R, Zhang C, Syed TN, Wang B and Zhou R (2024) Plastic pollution in agriculture as a threat to food security, the ecosystem, and the environment: an overview. *Agronomy* **14**, 548.

Li S, Kang S, Li F, Zhang L and Zhang B (2008) Vineyard evaporative fraction based on eddy covariance in an arid desert region of Northwest China. *Agricultural Water Management* **95**, 937–948.

Li M, Yan H, Zhang C, Zhang J, Wang G and Acquah SJ (2024) Current deficiencies and needed enhancements on greenhouse crop evapotranspiration models. *Journal of Drainage and Irrigation Machinery Engineering* **42**, 57–63.

Liu Z (2021) The accuracy of temporal upscaling of instantaneous evapotranspiration to daily values with seven upscaling methods. *Hydrology and Earth System Sciences* **25**, 4417–4433.

Liu G, Liu Y and Xu D (2011) Investigation on performance of evapotranspiration temporal upscaling methods based on eddy covariance measurements. *Transactions of the Chinese Society of Agricultural Engineering* **27**, 7–12.

Liu G, Hafeez M, Liu Y, Xu D and Vote C (2012a) A novel method to convert daytime evapotranspiration into daily evapotranspiration based on variable canopy resistance. *Journal of Hydrology* **414–415**, 278–283.

Liu G, Liu Y, Hafeez M, Xu D and Vote C (2012b) Comparison of two methods to derive time series of actual evapotranspiration using eddy covariance measurements in the southeastern Australia. *Journal of Hydrology* **454–455**, 1–6.

Liu X, Yang S, Xu J, Zhang J and Liu J (2017) Effects of soil heat storage and phase shift correction on energy balance closure of paddy fields. *Atmósfera* **30**, 39–52.

Liu X, Xu J, Zhou X, Wang W and Yang S (2020) Evaporative fraction and its application in estimating daily evapotranspiration of water-saving irrigated rice field. *Journal of Hydrology* **584**, 124317.

Liu Y, Jiang Q, Wang Q, Jin Y, Yue Q, Yu J, Zheng Y, Jiang W and Yao X (2022) The divergence between potential and actual evapotranspiration: an insight from climate, water, and vegetation change. *Science of the Total Environment* **807**, 150648.

Ma Z, Yan N, Wu B, Stein A, Zhu W and Zeng H (2019) Variation in actual evapotranspiration following changes in climate and vegetation cover during an ecological restoration period (2000–2015) in the Loess Plateau, China. *Science of the Total Environment* **689**, 534–545.

Ma Z, Wu B, Yan N, Zhu W and Xu J (2021) Coupling water and carbon processes to estimate field-scale maize evapotranspiration with Sentinel-2 data. *Agricultural and Forest Meteorology* **306**, 108421.

Malek E, Bingham GE and Mccurdy GD (1992) Continuous measurement of aerodynamic and alfalfa canopy resistances using the Bowen ratio-energy balance and Penman–Monteith methods. Boundary-Layer Meteorology **59**, 187–194.

Miralles DG, De Jeu RAM, Gash JH, Holmes TRH and Dolman AJ (2011) Magnitude and variability of land evaporation and its components at the global scale. *Hydrology and Earth System Sciences* **15**, 967–981.

Mu Q, Zhao M and Running SW (2011) Improvements to a MODIS global terrestrial evapotranspiration algorithm. *Remote Sensing of Environment* **115**, 1781–1800.

Ohmura A (1982) Objective criteria for rejecting data for Bowen ratio flux calculations. *Journal of Applied Meteorology* **21**, 595–598.

Perez PJ, Lecina S, Castellvi F, Martínez-Cob A and Villalobos FJ (2005) A simple parameterization of bulk canopy resistance from climatic variables for estimating hourly evapotranspiration. *Hydrological Processes* **20**, 515–532.

Pozníková G, Fischer M, van Kesteren B, Orság M, Hlavinka P, Žalud Z and Trnka M (2018) Quantifying turbulent energy fluxes and evapotranspiration in agricultural field conditions: a comparison of micrometeorological methods. *Agricultural Water Management* **209**, 249–263.

Shuttleworth W, Gurney R, Hsu A and Ormsby J (1989) FIFE: the variation in energy partition at surface flux sites. *IAHS Publication* **186**, 523–534.

Sugita M and Brutsaert W (1991) Daily evaporation over a region from lower boundary layer profiles measured with radiosondes. *Water Resources Research* **27**, 747–752.

Suleiman A and Crago R (2004) Hourly and daytime evapotranspiration from grassland using radiometric surface temperatures. *Agronomy Journal* **96**, 384–390.

Tang R and Li ZL (2017) An improved constant evaporative fraction method for estimating daily evapotranspiration from remotely sensed instantaneous observations. *Geophysical Research Letters* **44**, 2319–2326.

Tang R, Li Z-L and Sun X (2013) Temporal upscaling of instantaneous evapotranspiration: an intercomparison of four methods using eddy covariance measurements and MODIS data. *Remote Sensing of Environment* **138**, 102–118.

Tang R, Li ZL, Sun X and Bi Y (2017) Temporal upscaling of instantaneous evapotranspiration on clear-sky days using the constant reference evaporative fraction method with fixed or variable surface resistances at two cropland sites. *Journal of Geophysical Research: Atmospheres* **122**, 784–801.

Thom A (1972) Momentum, mass and heat exchange of vegetation. *Journal of the Royal Meteorological Society* **98**, 124–134.

Van Niel TG, McVicar TR, Roderick ML, van Dijk AIJM, Renzullo LJ and van Gorsel E (2011) Correcting for systematic error in satellite-derived latent heat flux due to assumptions in temporal scaling: assessment from flux tower observations. *Journal of Hydrology* **409**, 140–148.

Van Niel TG, McVicar TR, Roderick ML, van Dijk AIJM, Beringer J, Hutley LB and van Gorsel E (2012) Upscaling latent heat flux for thermal remote sensing studies: comparison of alternative approaches and correction of bias. *Journal of Hydrology* **468–469**, 35–46.

Wandera L, Mallick K, Kiely G, Roupsard O, Peichl M and Magliulo V (2017) Upscaling instantaneous to daily evapotranspiration using modelled daily shortwave radiation for remote sensing applications: an artificial neural network approach. *Hydrology and Earth System Sciences* **21**, 197–215.

Wang B, Bao R, Yan H, Zheng H, Wu J, Zhang C and Wang G (2024a) Study of evapotranspiration and crop coefficients for eggplant in a Venlo-type greenhouse in South China. *Irrigation and Drainage.*

Wang B, Yan H, Zheng H, Wu J, Tian D, Zhang C, Zhu X, Wang G, Lakhiar IA and Liu Y (2024b) Estimation of latent heat flux of pasture and maize in arid region of Northwest China based on canopy resistance modeling. *Frontiers in Environmental Science* **12**, 1397704.

Xu T, Liu S, Xu L, Chen Y, Jia Z, Xu Z and Nielson J (2015) Temporal upscaling and reconstruction of thermal remotely sensed instantaneous evapotranspiration. *Remote Sensing* **7**, 3400–3425.

Xu X, Li X, Wang X, He C, Tian W, Tian J and Yang L (2020) Estimating daily evapotranspiration in the agricultural-pastoral ecotone in Northwest China: a comparative analysis of the complementary relationship, WRF-CLM4.0, and WRF-Noah methods. *Science of the Total Environment* **729**, 138635.

Yan H, Zhang C, Coenders Gerrits M, Acquah SJ, Zhang H, Wu H, Zhao B, Huang S and Fu H (2018) Parametrization of aerodynamic and canopy resistances for modeling evapotranspiration of greenhouse cucumber. *Agricultural and Forest Meteorology* **262**, 370–378.

Yan H, Acquah SJ, Zhang C, Wang G, Huang S, Zhang H, Zhao B and Wu H (2019) Energy partitioning of greenhouse cucumber based on the application of Penman-Monteith and bulk transfer models. *Agricultural Water Management* **217**, 201–211.

Yan H, Yu J, Zhang C, Wang G, Huang S and Ma J (2021) Comparison of two canopy resistance models to estimate evapotranspiration for tea and wheat in southeast China. *Agricultural Water Management* **245**, 106581.

Yan H, Huang S, Zhang J, Zhang C, Wang G, Li L, Zhao S, Li M and Zhao B (2022a) Comparison of Shuttleworth–Wallace and dual crop coefficient method for estimating evapotranspiration of a tea field in Southeast China. *Agriculture* **12**, 1392.

Yan H, Li M, Zhang C, Zhang J, Wang G, Yu J, Ma J and Zhao S (2022b) Comparison of evapotranspiration upscaling methods from instantaneous to daytime scale for tea and wheat in southeast China. *Agricultural Water Management* **264**, 107464.

Yan H, Deng S, Zhang C, Wang G, Zhao S, Li M, Liang S, Jiang J and Zhou Y (2023) Determination of energy partition of a cucumber grown venlo-type greenhouse in southeast China. *Agricultural Water Management* **276**, 108047.

Yang D-W, Chen H and Lei H-M (2013) Analysis of the diurnal pattern of evaporative fraction and its controlling factors over croplands in the Northern China. *Journal of Integrative Agriculture* **12**, 1316–1329.

Yang P, Hu H, Tian F, Zhang Z and Dai C (2016) Crop coefficient for cotton under plastic mulch and drip irrigation based on eddy covariance observation in an arid area of northwestern China. *Agricultural Water Management* **171**, 21–30.

Zhang BZ, Kang SZ, Zhang L, Du TS, Li SE and Yang XY (2010) Estimation of seasonal crop water consumption in a vineyard using Bowen ratio-energy balance method. *Hydrological Processes* **21**, 3635–3641.

Zhang B, Chen H, Xu D and Li F (2017) Methods to estimate daily evapotranspiration from hourly evapotranspiration. *Biosystems Engineering* **153**, 129–139.

Zhang Y, Kong D, Gan R, Chiew FHS, McVicar TR, Zhang Q and Yang Y (2019) Coupled estimation of 500 m and 8-day resolution global evapotranspiration and gross primary production in 2002–2017. *Remote Sensing of Environment* **222**, 165–182.

Zhao S, Yan H, Zhang C, Li M, Deng S, Liang S and Jiang J (2023) Estimation of cucumber evapotranspiration in greenhouse based on improved dual crop coefficient model and Priestley-Taylor model. *Journal of Drainage and Irrigation Machinery Engineering* **41**, 849–857.